

Banner appropriate to article type will appear here in typeset article

A local intermittency based Reynolds-averaged transition model for turbulent mixing induced by interfacial instabilities

Hansong Xie¹, Mengjuan Xiao², Yousheng Zhang^{1,2}† and Yaomin Zhao^{1,3}‡

¹HEDPS, Center for Applied Physics and Technology, and College of Engineering, Peking University, Beijing 100871, China

²Institute of Applied Physics and Computational Mathematics, Beijing 100094, China

³State Key Laboratory for Turbulence and Complex Systems, College of Engineering, Peking University, Beijing 100871, China

(Received xx; revised xx; accepted xx)

Accurate prediction of mixing transition induced by interfacial instabilities is vital for engineering applications, but has remained a great challenge for decades. For engineering practices, Reynolds-averaged Navier-Stokes simulation (RANS) is the most viable method. However, existing RANS models for mixing problems are mostly designed for fully developed turbulence, failing to depict the locally spatio-temporal-dependent characteristic of transition. In the present study, the idea of the intermittent factor (denoted as γ), which has been widely used in boundary layer transition in aerospace engineering, is extended to the mixing problems. Specifically, a transport equation for γ is built based on local flow variables, which is used to describe the locally spatio-temporal-dependent characteristic of transition. Furthermore, γ is coupled into the widely used K-L turbulent mixing model to constrain the two key product sources terms that dominate the evolution of mixing, i.e. the Reynolds stress and the buoyancy effect. Subsequently, the simulations of two reshocked Richtmyer-Meshkov mixing cases with remarkable transition effects confirm that the proposed model has a good performance for predicting mixing transition. To the best of our knowledge, it is the first study that an extra transport equation for intermittent factor has been proposed for a RANS mixing transition model. More importantly, the present modeling framework is flexible and has the potential to be applied to other RANS models. It provides a promising strategy for more advanced modeling for mixing transition.

Key words:

† Email address for correspondence: zhang_yousheng@iapcm.ac.cn

‡ Email address for correspondence: yaomin.zhao@pku.edu.cn

1. Introduction

Rayleigh-Taylor, Richtmyer-Meshkov and Kelvin-Helmholtz instabilities are crucial in a wide range of natural phenomena and engineering applications, such as supernova explosion (Burrows 2000), inertial confinement fusion (Thomas & Kares 2012), and so on. In practical flows, these instabilities frequently interact with each other and cause mixing between different materials. Therefore, accurate prediction of mixing is of great significance for understanding natural phenomena and optimizing engineering applications. Three primary methodologies are utilized to numerically predict the evolution of mixing: direct numerical simulation, large eddy simulation (LES), and Reynolds-averaged Navier-Stokes simulation (RANS). Specifically, RANS is widely applied in engineering owing to its computational efficiency.

The mixing evolution generally goes through three stages: development of instability, mixing transition and turbulent mixing. In the first stage, hydrodynamic instabilities amplify perturbations at the interface, leading to a continuous increment of the interface area. The instability development during this stage is characterized as linear or weakly nonlinear, owing to the small perturbation amplitudes. Thus accurate prediction can be achieved through analytical theories or numerical simulations (Liu *et al.* 2022; Zhang & Guo 2022; Mikaelian 1998; Layzer 1955). Perturbations dominate the flow in the first stage, until the amplitude of interface perturbations becomes comparable to the dominant wavelength. As the flow transitions to the second stage, the interfacial structures start to break into smaller scales, and multiscale behaviour appears due to the coupling and competition between different modes. Subsequently, the flow in the third stage evolves into a well-mixed state and displays self-similarity and deterministic statistical laws, making it suitable for RANS modeling (Zhang *et al.* 2020; Dimonte & Tipton 2006; Kokkinakis *et al.* 2015). Unlike the first and third stages, which can be reasonably well predicted utilizing current methodologies, the profoundly nonlinear dynamics encountered in the intermediate mixing transition stage pose formidable challenges for modeling endeavors. Specifically, the mixing transition is a temporal evolutionary process characterized by pronounced spatial variations in different locations. This locally spatio-temporally dependent characteristic cannot be accurately captured by existing RANS mixing models, which are typically proposed for fully developed turbulent flows.

For accurate prediction of transition, two key aspects need to be considered. Firstly, it is essential to accurately identify the onset of transition. Based on observations from a series of flows, Dimotakis (2000) proposed a transition threshold based on the outer-scale Reynolds number, approximately at $Re = 1 \sim 2 \times 10^4$. This threshold for transition is established based on the appearance of an inertial range, marking an abrupt transition from a low-mixed state to a well-mixed state. It demonstrates that this threshold actually corresponds to the ultimate Reynolds number attained at the end of the transition. Zhou *et al.* (2003) extended Dimotakis's criterion to the mixing problem by introducing an additional length scale that evolves with time. Notably, the aforementioned criteria, depending on the identification of inertial range, can only be applied *a posteriori*, failing to meet the requirement of real-time predictions. Moreover, the corresponding transition threshold value relies on the outer Reynolds number, which is essentially a global quantity unable to capture the local characteristics of the transition. Recently, Wang *et al.* (2022) proposed a new transition criterion based on mixing mass, enabling identification of transition onset and cessation times. Nonetheless, the mixing mass remains a global parameter, rendering it unsuitable for real-time RANS predictions.

Secondly, accurate prediction of the subsequent flow development after the onset of transition is crucial. Given that most of the existing RANS mixing models are constructed under the assumption of fully developed turbulence, utilizing these models directly to predict

transition would result in an overestimation of the mixing evolution. To employ RANS models for predicting transitions, Haines *et al.* (2013) artificially controlled the moment of switching on the turbulence model, based on the timing of shock waves impacting on the interface. While this approach successfully predicts the evolution of mixing transition, it has an empirical nature. A more effective strategy would be to enable the model to automatically characterize the onset and evolution of transition. To achieve a precise depiction of the transition process, Grinstein *et al.* (2020) proposed a dynamic hybrid RANS/LES bridging approach, aiming to utilize LES information to improve RANS predictions. Despite the method's promising potential, it remains nascent and needs further refinement prior to its suitability for engineering applications.

As previously mentioned, the actual transition process exhibits significant local spatio-temporal dependence, necessitating that RANS models possess the capability to capture this characteristic. It is well known that the intermittent factor γ , widely employed for boundary layer transition phenomena in aerospace engineering, can reflect this characteristic and is widely used to describe variations of flow states. Nevertheless, no research has been reported applying this well-developed idea to mixing problems. Therefore, in this study we extend the concept of the intermittent factor to mixing flows and develop a RANS mixing transition model. As demonstrated later, the current strategy proves to be effective.

The paper is organized as follows. Section 2 provides a detailed documentation of the modeling process, encompassing the governing equations and the baseline model in Section 2.1, the key modeling idea in Section 2.2, and the construction of the transport equation for γ in Section 2.3. Section 3 validates the proposed model using two representative cases. Finally, Section 4 summarizes the current study and presents further discussions.

2. Methodology

2.1. Governing equations and baseline model

The multicomponent RANS equations are solved considering molecular transport and thermodynamic coefficients. The transport equations for the mean density ρ , velocity u_i , total energy E of the mixture, and mass fraction Y_α of specie α are given as follows:

$$\frac{\partial \bar{\rho}}{\partial t} + \frac{\partial \bar{\rho} \tilde{u}_j}{\partial x_j} = 0, \quad (2.1)$$

$$\frac{\partial \bar{\rho} \tilde{u}_i}{\partial t} + \frac{\partial \bar{\rho} \tilde{u}_i \tilde{u}_j}{\partial x_j} + \frac{\partial \bar{p}}{\partial x_i} = -\frac{\partial \tau_{ij}}{\partial x_j} + \frac{\partial \bar{\sigma}_{ij}}{\partial x_j}, \quad (2.2)$$

$$\frac{\partial \bar{\rho} \tilde{E}}{\partial t} + \frac{\partial (\bar{\rho} \tilde{E} + \bar{p}) \tilde{u}_j}{\partial x_j} = D_E + D_K + \frac{\partial}{\partial x_j} (-\tau_{ij} \tilde{u}_i + \bar{\sigma}_{ij} \tilde{u}_i - \bar{q}_c - \bar{q}_d), \quad (2.3)$$

$$\frac{\partial \bar{\rho} \tilde{Y}_\alpha}{\partial t} + \frac{\partial \bar{\rho} \tilde{Y}_\alpha \tilde{u}_j}{\partial x_j} = \frac{\partial}{\partial x_j} \left(-\bar{\rho} \overline{u_i'' Y_\alpha''} + \bar{\rho} \bar{D} \frac{\partial \tilde{Y}_\alpha}{\partial x_j} \right). \quad (2.4)$$

The overbar and tilde symbols represent the Reynolds and Favre averaged fields, respectively. The double prime symbol denotes Favre fluctuations. The heat flux \bar{q}_c is defined by the Fourier's law as $\bar{q}_c = -\bar{\kappa} \partial \bar{T} / \partial x_j$. The interspecies diffusional heat flux \bar{q}_d is given by $\bar{q}_d = -\sum \bar{\rho} \bar{D} C_{p\alpha} \bar{T} \partial \tilde{Y}_\alpha / \partial x_j$. The viscous stress tensor is given as

$$\bar{\sigma}_{ij} = 2\bar{\mu} (\tilde{S}_{ij} - \tilde{S}_{kk} \delta_{ij} / 3), \quad \tilde{S}_{ij} = (\partial \tilde{u}_i / \partial x_j + \partial \tilde{u}_j / \partial x_i) / 2. \quad (2.5)$$

Here $\bar{\mu}$, \bar{D} , $\bar{\kappa}$, and $C_{p\alpha}$ represent dynamic viscosity, mass diffusivity, thermal conductivity, and constant-pressure specific heat of specie α , respectively. Moreover, τ_{ij} is the Reynolds

stress, and the terms $D_E = -\partial(\overline{\rho u_j'' e''} + \overline{p u_j''})/\partial x_j$, $D_K = -\partial(\overline{\rho u_i'' u_i'' u_j''}/2)/\partial x_j$, and $-\overline{\rho u_i'' Y_\alpha''}$ represent the turbulent diffusion terms of the total energy, turbulent kinetic energy (TKE) \tilde{K} , and mass fraction, respectively. It should be emphasized that Eqs.(2.1)~(2.4) are deduced based on the concept of ensemble averaging and are theoretically applicable to the three stages of mixing evolution. Once the unclosed terms are appropriately modeled, the equation array can be solved by coupling it with the equation of state (EOS) $\bar{p}M = \bar{\rho}R\tilde{T}$ for the perfect gas, where M and R denoting the molar mass and the gas constant, respectively. The EOS for the mixture is calculated under the assumptions of iso-temperature and partial-pressure. Additionally, the fluid properties of the mixture are determined using a species-linearly weighted assumption (Livescu 2013).

In previous studies, the majority of RANS simulations focus on fully developed turbulence. Consequently, numerous turbulent mixing models have been proposed, including the K- ϵ , K-L, K-L-a, and Besnard-Harlow-Rauenzahn (BHR) models. In this study we take the well-developed K-L model as an example to briefly illustrate how turbulent flow is modeled. Specifically, the turbulent transport terms are modeled by the gradient diffusion assumption (GDA)

$$-\overline{\rho u_i'' f''} = \frac{\mu_t}{N_f} \frac{\partial \tilde{f}}{\partial x_i}, \quad (2.6)$$

where f denotes an arbitrary physical variable and N_f is a model coefficient. The symbol μ_t is the turbulent viscosity, which is described by the TKE \tilde{K} and the turbulent length scale \tilde{L}

$$\mu_t = C_\mu^R \bar{\rho} \tilde{L} \sqrt{2\tilde{K}}. \quad (2.7)$$

Here C_μ^R is a model coefficient, which is calculated based on the realizability principle (Xiao *et al.* 2021). With the Boussinesq eddy viscosity hypothesis, the Reynolds stress is modeled as

$$\tau_{ij} = C_P \bar{\rho} \tilde{K} \delta_{ij} - 2\mu_t (\tilde{S}_{ij} - \tilde{S}_{kk} \delta_{ij}/3), \quad (2.8)$$

where C_P is a model coefficient. Additionally, the closed transport equations of the TKE and \tilde{L} are

$$\frac{\partial \bar{\rho} \tilde{K}}{\partial t} + \frac{\partial \bar{\rho} \tilde{u}_j \tilde{K}}{\partial x_j} = -\tau_{ij} \frac{\partial \tilde{u}_i}{\partial x_j} + \frac{\partial}{\partial x_j} \left(\frac{\mu_t}{N_K} \frac{\partial \tilde{K}}{\partial x_j} \right) + S_{Kf} - C_D \bar{\rho} \left(\sqrt{2\tilde{K}} \right)^3 / \tilde{L}, \quad (2.9)$$

$$\frac{\partial \bar{\rho} \tilde{L}}{\partial t} + \frac{\partial \bar{\rho} \tilde{u}_j \tilde{L}}{\partial x_j} = \frac{\partial}{\partial x_j} \left(\frac{\mu_t}{N_L} \frac{\partial \tilde{L}}{\partial x_j} \right) + C_L \bar{\rho} \sqrt{2\tilde{K}} + C_C \bar{\rho} \tilde{L} \frac{\partial \tilde{u}_j}{\partial x_j}, \quad (2.10)$$

where S_{Kf} is the buoyancy product term. More details about the K-L model, including the value of the model coefficients and the expression of S_{Kf} , can be found in Zhang *et al.* (2020). Nevertheless, the aforementioned K-L model is not suitable for the mixing transition stage since all closures are developed for fully developed turbulence. The next two sections will introduce how to construct the mixing transition model on the basis of the baseline K-L model.

2.2. Modeling strategy for the mixing transition model

In the transition process, the flow state undergoes dramatic variations and exhibits significant local spatio-temporal dependence. Hence, it is necessary to seek for a suitable flow variable to capture this characteristic. Exactly, this aligns with the concept of the intermittent factor γ , which has been extensively employed to predict boundary layer transitions in aerospace engineering. Therefore, in this study we extend the idea of the intermittent factor to mixing problems.

It is important to note that the γ in the boundary layer is often defined based on the time-averaged operations because of the statistically stationary nature, which cannot be directly applied to the unsteady mixing flows. Consequently, following the original definition (Dopazo 1977), the concept of the intermittent factor is defined using the ensemble-averaged approach. Specifically, we define the intermittent function $I(x, y, z, t, n)$, which takes into account time and space variables, as well as the sample parameter n . Thus, for a given sample, the flow state at a specified spatio-temporal point is either laminar or turbulent. We further assign $I = 0$ for laminar flow and $I = 1$ for turbulence. With the ensemble-averaged approach, the intermittent factor is defined as

$$\gamma \equiv \frac{1}{N} \sum_{n=1}^N I(x, y, z, t, n) = \gamma(x, y, z, t), \quad (2.11)$$

where N represents the sample size.

The Reynolds stress plays a crucial role in the transition to turbulence. However, the existing closure is only applicable to turbulent flows, thus necessitating remodeling. In accordance with the definition (2.11), we express the new Reynolds stress τ_{ij}^{new} as

$$\tau_{ij}^{new} = (1 - \gamma)\tau_{ij}^{lam} + \gamma\tau_{ij}^{tur}. \quad (2.12)$$

Here τ_{ij}^{lam} and τ_{ij}^{tur} represent the Reynolds stresses associated with the laminar and turbulent states, respectively, with τ_{ij}^{lam} being negligible. Thus the new Reynolds stress is only related to the component of the turbulent state τ_{ij}^{tur} , which is closed by Eq.(2.8). Given that the normal stress component of the Reynolds stress can be determined by TKE, γ is only applied to the turbulent viscosity μ_t to modify the deviatoric stress part, i.e.

$$\tau_{ij}^{new} = C_P \bar{\rho} \tilde{K} \delta_{ij} - 2\mu_{new}(\tilde{S}_{ij} - \tilde{S}_{kk}\delta_{ij}/3), \quad \mu_{new} = \gamma\mu_t = C_\mu^R \gamma \bar{\rho} \tilde{L} \sqrt{2\tilde{K}}. \quad (2.13)$$

Accordingly, in the turbulent diffusion term modeled by the GDA, μ_t is replaced by μ_{new} .

In addition to the Reynolds stress, the buoyancy product term S_{Kf} in Eq.(2.9) is also crucial for the mixing evolution, which also requires further improvement for the mixing transition stage. To modify the baseline model minimally, the simplest approach is multiplying S_{Kf} by γ . Nevertheless, this treatment may cause that the TKE cannot be excited especially for the initial stage of instability due to the quite small value of the intermittent factor γ . Therefore, it is suggested to introduce a small excitation source denoted as $\zeta = 1 \times 10^{-9}$ into the buoyancy product term, which dominates the production of TKE. Thus the new buoyancy product term S_{Kf}^{new} is expressed as

$$S_{Kf}^{new} = \max(\gamma, \zeta) S_{Kf}. \quad (2.14)$$

2.3. Transport equation for the intermittent factor

Sec.2.2 presents the two key improvements in constructing the mixing transition model. In this section, the transport equation for γ is built to describe the local spatio-temporal dependence of the the mixing transition flow and improve the generalization performance of the models.

Following the framework (Wang & Fu 2011) of constructing the boundary layer transition models based on the intermittent factor, we present the transport equation for γ :

$$\frac{\partial \bar{\rho} \gamma}{\partial t} + \frac{\partial \bar{\rho} \tilde{u}_j \gamma}{\partial x_j} = \frac{\partial}{\partial x_j} \left[\left(\bar{\mu} + \frac{\mu_{eff}}{N_\gamma} \right) \frac{\partial \gamma}{\partial x_j} \right] + P_\gamma - \epsilon_\gamma. \quad (2.15)$$

Here P_γ and ϵ_γ represent the product and dissipation terms, respectively. The model

coefficient N_γ is set to 1. The physical process of mixing evolution tells that the flow eventually reaches a fully-developed turbulent state, indicating that the Reynolds stress τ_{ij}^{new} and the buoyancy product term S_{Kf}^{new} should ultimately approach the closed form in the baseline K-L turbulent model. Correspondingly, γ should monotonically increase to 1 until the flow becomes fully developed turbulence. This implies that $P_\gamma - \epsilon_\gamma$ should be greater than 0 to provide a positive net increment. To meet this requirement, we adopt the simplest approach of setting $\epsilon_\gamma = \gamma P_\gamma$.

A transition model must have two basic functions: identifying the onset of transition and predicting the subsequent flow evolution accurately. In the current model, these functions are represented as:

$$P_\gamma = F_{onset} G. \quad (2.16)$$

Here F_{onset} serves as a transition switch, while G describes the growth rate of γ . The expression for F_{onset} is given by

$$F_{onset} = 1 - \exp\left(-\frac{C\tilde{L}\sqrt{2\tilde{K}}/\nu}{Re_{tra}} \sqrt{\frac{|\nabla E_u|}{|\nabla \tilde{K}|}}\right). \quad (2.17)$$

In this equation, ν and E_u represent the molecular kinematic viscosity and the mean kinetic energy respectively, while C is a model coefficient and Re_{tra} corresponds to the ultimate Reynolds number attained at the end of the transition stage, taken as 10^4 (Dimotakis 2000). Eq.(2.17) is easy to understand with the following explanation. Through an analysis of the order, the exponent part in Eq.(2.17) can be expressed as $C\tilde{L}\tilde{u}/\nu Re_{tra}$, which is further simplified as Re_{local}/Re_{tra} . It is evident that when the flow remains stagnant or the turbulence is weak, Re_{local} approaches 0, resulting in $F_{onset} \rightarrow 0$, which means that transition does not occur. Consequently, the intermittent factor does not grow. As instabilities develop and fluctuations intensify, mixing begins to evolve. Once the ratio between the local Reynolds number Re_{local} and the ultimate Reynolds number Re_{tra} surpasses a certain threshold value, the model identifies the occurrence of transition. Although there may not be an universal value for the critical ratio across different problems, 0.01 is a relatively reasonable order. Based on the analysis of the order, the coefficient C should be of the order 1, and specifically, it is set to 5 in the present study.

Furthermore, the growth rate of the intermittent factor γ is described using the function G . Since there are no relevant studies available as a reference, we adopt the growth rate of the intermittent factor in boundary layer as a basis. Accordingly, G is expressed as:

$$G = \bar{\rho} S \gamma^{0.5} (1 - \gamma). \quad (2.18)$$

Here S represents the amplitude of the mean strain rate, defined as $S = \sqrt{2\tilde{S}_{ij}\tilde{S}_{ij}}$.

3. Model validation

In this section, the performance of the proposed model is verified by two representative reshocked RM mixing cases, which originate from the experiments conducted at the linear shock tube facility of AWE (Aldermaston). Fig.1(a) represents the inverse chevron case (noted as case A) in Hahn *et al.* (2011), which features a dense SF6 gas block encased in air within a tube. Moreover, Fig.1(b) represents the shock tube experiments (noted as case B) reported in Bates *et al.* (2007), in which shock waves interact with a half-height rectangular block of dense SF6 gas. In both cases, apart from the RM effect, the special interface design leads to an initial KH instability that promotes the transition to turbulence. Additionally, due to the presence of reflective boundary, the reflected shock wave from the right wall

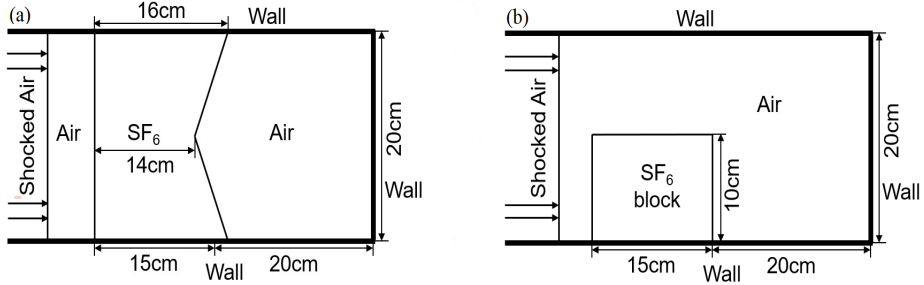


Figure 1: Schematic diagrams of the two reshocked RM mixing cases.

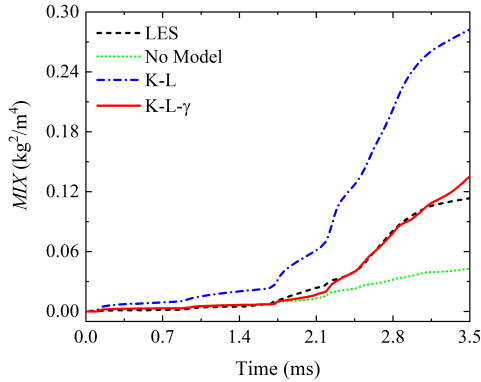


Figure 2: Total mixing (MIX) vs time for the inverse chevron case A.

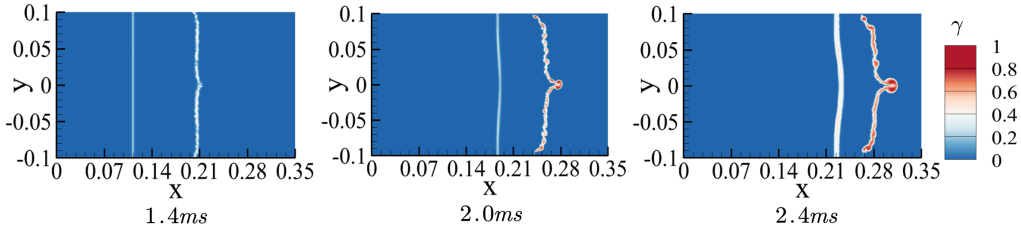


Figure 3: Contours of the γ at three different moments. The subfigures from left to right represent the moments before the first reshocking ($1.4ms$), between the first and the second reshocking ($2.0ms$), and after the second reshocking ($2.4ms$), respectively.

will reshock the mixing region to enhance the mixing and make the transition effect more conspicuous.

Because both of the cases have a good two-dimensional (2-D) statistical characteristic, the present RANS calculations are set as 2-D. The numerical scheme employed is the same as that used in Xiao *et al.* (2022), with the exception of setting the Courant-Friedrichs-Lewy (CFL) number to 0.05 to enhance computational robustness. Uniform grids are adopted for both cases, with grid scales Δx set to $1/16cm$ and $1/8cm$ for case A and B, respectively. Near the interfaces, the initial turbulent length scale \bar{L} and intermittency factor γ are specified as $0.055cm$ and 0 for case A. For case B the initial \bar{L} is set to $0.015cm$, and γ is set to 1 due to its faster transition process than case A.

For mixing flows, the integral quantity MIX is not prone to statistical noise and is a simple

and effective way to measure variations of the total amount of mixing in complex flows (Hahn *et al.* 2011). The calculation of MIX is given by:

$$MIX = \int \bar{\rho}^2 \bar{Y}_1 \bar{Y}_2 dV, \quad (3.1)$$

where \bar{Y}_1 and \bar{Y}_2 represent the mass fractions of the two species, with $\bar{Y}_1 = 1 - \bar{Y}_2$. For three-dimensional (3-D) simulations $dV = dx dy dz$, whereas for 2-D simulations, $dV = dx dy$.

Fig.2 illustrates the temporal evolution of MIX for the inverse chevron case. The 3-D LES is implemented using the explicit subgrid stress model recently proposed by Xiao *et al.* (2022), which shows a good predictive accuracy for mixing problems induced by interfacial instabilities. To make the 2-D and 3-D simulations comparable, the results of LES are obtained by firstly averaging the 3-D flow field along the spanwise direction, and then calculating the MIX based on (3.1). More discussions about the results of the LES will be published separately. In addition, two additional simulations are conducted to highlight the effect of the proposed model (K-L- γ), one of which not including any model (No Model) and the other using the baseline K-L model.

Fig.2 shows that, at approximately $0.1ms$ and $0.85ms$, the incident shock wave successively impacts on the planar and chevron interfaces, resulting in a slight increase in MIX . At around $1.7ms$, a sudden growth in total mixing occurs when the mixing region is firstly reshocked by the reflected wave. Subsequently, around $2.2ms$, the mixing region is reshocked again, leading to a rapid rise in MIX . The evolutionary process observed and the results of LES indicate that prior to reshocking, the mixing is at a low-mixed level. Consequently, the flow should be characterized as laminar or low-turbulent, which is accurately represented by the γ contour at $1.4ms$ in Fig.3, where γ exhibits consistently small values throughout the entire mixing region. Quantitatively, the K-L- γ model also effectively predict the low-mixed state while the baseline model overpredicts the mixing evolution. After the mixing region is reshocked by the reflected wave, the flow undergoes a significant transition phase, during which the onset of transition is accurately identified by the K-L- γ model. Subsequently, the turbulence intensity enhances dramatically, and γ promptly responds to these flow variations, exhibiting larger amplitudes within the mixing region, as shown in the contour at $2.0ms$ in Fig.3. After the second reshocking event, the mixing enters a high-turbulent and well-mixed state. Such a flow variation is visually depicted by the contour of γ at $2.4ms$ in Fig.3, where γ has a larger value and the mixing region become wider. The abovementioned mixing evolution is predicted accurately by the K-L- γ model, demonstrating a good agreement with the LES results. Conversely, the K-L model presents an absurd overprediction.

Fig.4(a) further compares the evolution of distances between the end wall and the characteristic bubble and spike structures, which are tracked based on the mass fraction 0.5 at the down wall (left edge of the wall-bubble) and the SF6 mass fraction 0.1 (the tip of spike). Results indicate that all the simulations accurately capture the location evolution of the spike's tip. Although the bubble position is difficult to predict, the proposed K-L- γ model has a significantly better performance than the baseline model.

The shock tube case shown in Fig.1(b) is used to assess the generalization performance of the proposed model. Fig.4(b) shows the evolutions of the maximum extends of the SF6 block along the x and y directions. The experimental results are presented as error bands, while the Adaptive Mesh Refinement (AMR) results are extracted from the high-resolution simulation conducted by Bates *et al.* (2007). The locations of the left, right and top sides of the SF6 block are determined based on the volume fraction of 0.1. Fig.4(b) indicates that the predictions of the K-L- γ model largely fall within the error band provided by the experiment, demonstrating a significant improvement over the baseline K-L model. Notably, around $1.6ms$, there is a noteworthy disparity between the predictions of the two RANS

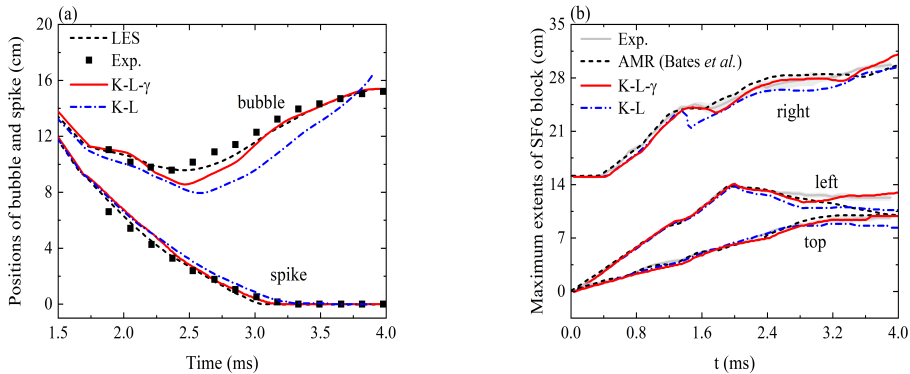


Figure 4: (a) Distances of the characteristic spike and bubble from the end wall for case A.
 (b) Evolution of extends of the SF6 block along the x and y directions for case B.

models with respect to the right position of the SF6 block. At this moment, the mixing region encounters a reshocking, which promotes the transition behaviour. The reshocking caused by the reflected wave compresses the mixing region, leading to a shift of the SF6 block towards the left side. The experimental and AMR results indicate that the compression process is weak, as observed from the minimal variation in the right extent of the SF6 block. The present K-L- γ model reasonably captures this compression behaviour and accurately predicts the evolution of the mixing transition stage. In contrast, the K-L model performs poorly.

4. Conclusions and discussions

The local spatio-temporal dependence of mixing transition requires that RANS models possess the corresponding capability to describe this characteristic. Inspired by the intermittent factor widely used in boundary layer transition within the aerospace field, this study extends this well-developed modeling strategy to the mixing problems induced by interfacial instabilities. Specifically, the concept of the intermittent factor γ is defined based on the ensemble-averaged approach, and a transport equation is built for it. Subsequently, taking the well-developed K-L turbulent mixing model as an example, we couple the γ equation into the K-L model to modify the two key source terms that dominate the mixing evolution, i.e. the Reynolds stress and buoyancy product terms. To validate the performance of the proposed model, two representative reshocked RM mixing cases are examined. The good predictive results demonstrate that the present model can accurately capture the onset of the transition and depict its subsequent evolution. Furthermore, it exhibits the potential to provide accurate predictions for the entire process of mixing evolution.

To the best of our knowledge, it is the first study that an extra transport equation for intermittent factor has been proposed for a RANS mixing transition model. More importantly, the current modeling framework exhibits flexibility and demonstrates a promising potential for more advanced modeling strategies of mixing transition. It is expected that the present framework can be extended to other turbulent mixing models, such as the K- ϵ , BHR models, and so on.

Nonetheless, several challenges remain to be addressed. Firstly, additional cases are needed to extensively validate the performance of the proposed model. However, a scarcity of benchmark cases demonstrating notable transition effects exists, so further experiments and

high-resolution simulations are desired to mitigate this limitation. Secondly, the prediction for the *MIX* in Fig. 2 can be further improved, particularly during the initial stage of transition. This can be probably achieved by improving the model of Eq. (2.18) to describe the growth rate of γ .

Acknowledgements.

This work was supported by the National Natural Science Foundation of China (Grant Nos. 12222203, 92152102, 11972093).

Declaration of Interests.

The authors report no conflict of interest.

REFERENCES

- BATES, K. R., NIKIFORAKIS, N. & HOLDER, D. 2007 Richtmyer-Meshkov instability induced by the interaction of a shock wave with a rectangular block of SF₆. *Phys. Fluids* **19** (3), 036101.
- BURROWS, A. 2000 Supernova explosions in the Universe. *Nature* **403** (6771), 727–733.
- DIMONTE, G. & TIPTON, R. 2006 K-L turbulence model for the self-similar growth of the Rayleigh-Taylor and Richtmyer-Meshkov instabilities. *Phys. Fluids* **18** (8), 85101.
- DIMOTAKIS, P. E. 2000 The mixing transition in turbulent flows. *J. Fluid Mech.* **409**, 69–98.
- DOPAZO, C. 1977 On conditioned averages for intermittent turbulent flows. *J. Fluid Mech.* **81** (3), 433–438.
- GRINSTEIN, F. F., SAENZ, J. A., RAUENZAHN, R. M., GERMANO, M. & ISRAEL, D. M. 2020 Dynamic bridging modeling for coarse grained simulations of shock driven turbulent mixing. *Comput. Fluids* **199**, 104430.
- HAHN, M., DRIKAKIS, D., YOUNGS, D. L. & WILLIAMS, R. J. R. 2011 Richtmyer-Meshkov turbulent mixing arising from an inclined material interface with realistic surface perturbations and reshocked flow. *Phys. Fluids* **23** (4), 046101.
- HAINES, B. M., GRINSTEIN, F. F. & SCHWARZKOPF, J. D. 2013 Reynolds-averaged Navier-Stokes initialization and benchmarking in shock-driven turbulent mixing. *J. Turbul.* **14** (2), 46–70.
- KOKKINAKIS, I. W., DRIKAKIS, D., YOUNGS, D. L. & WILLIAMS, R. J. R. 2015 Two-equation and multi fluid turbulence models for Rayleigh-Taylor mixing. *Int. J. Heat Fluid Fl.* **56**, 233–250.
- LAYZER, D. 1955 On the instability of Superposed Fluids in a Gravitational Field. *Astrophys. J.* **122**, 1.
- LIU, C., ZHANG, Y. & XIAO, Z. 2022 A unified theoretical model for spatiotemporal development of Rayleigh-Taylor and Richtmyer-Meshkov fingers. *J. Fluid Mech.* **954**, A13.
- LIVESCU, D. 2013 Numerical simulations of two-fluid turbulent mixing at large density ratios and applications to the Rayleigh-Taylor instability. *Philos. Trans. R. Soc. A* **371** (2003), 20120185.
- MIKAEILIAN, K. O. 1998 Analytic Approach to Nonlinear Rayleigh-Taylor and Richtmyer-Meshkov Instabilities. *Phys. Rev. Lett.* **80**, 508–511.
- THOMAS, V. A. & KARES, R. J. 2012 Drive asymmetry and the origin of turbulence in an icf implosion. *Phys. Rev. Lett.* **109** (7), 075004–075004.
- WANG, L. & FU, S. 2011 Development of an Intermittency Equation for the Modeling of the Supersonic/Hypersonic Boundary Layer Flow Transition. *Flow Turbul. Combust.* **87** (1), 165–187.
- WANG, R., SONG, Y., MA, Z., MA, D., WANG, L. & WANG, P. 2022 The transition to turbulence in rarefaction-driven Rayleigh-Taylor mixing: Effects of diffuse interface. *Phys. Fluids* **34** (1), 015125.
- XIAO, M., HU, Z., DAI, Z. & ZHANG, Y. 2022 Experimentally consistent large-eddy simulation of re-shocked Richtmyer-Meshkov turbulent mixing. *Phys. Fluids* **34** (12), 125125.
- XIAO, M., ZHANG, Y. & TIAN, B. 2021 A K-L model with improved realizability for turbulent mixing. *Phys. Fluids* **33** (2), 022104.
- ZHANG, Q. & GUO, W. 2022 Quantitative theory for spikes and bubbles in the Richtmyer-Meshkov instability at arbitrary density ratios. *Phys. Rev. Fluids* **7**, 093904.
- ZHANG, Y., HE, Z., XIE, H., XIAO, M. & TIAN, B. 2020 Methodology for determining coefficients of turbulent mixing model. *J. Fluid Mech.* **905**, A26.
- ZHOU, Y., ROBAY, H. & BUCKINGHAM, A. 2003 Onset of turbulence in accelerated high-reynolds-number flow. *Phys. Rev. E* **67**, 056305.